ARTICLE
Journal of Cellular Biochemistry 106:1136–1145 (2009)

Journal of Cellular Biochemistry

Proteomic Analysis Reveals Upregulation of RKIP in S-180 Implanted BALB/C Mouse After Treatment With Ascorbic Acid

Seyeon Park,[1*] Eun Sook Ahn,[1] Sukchan Lee,[2] Manyong Jung,[2] Jin Hee Park,[2] Sang Yeop Yi,[3] and Chang-Hwan Yeom[4**]

[1]*Department of Applied Chemistry, Dongduk Women's University, Seoul, Korea*
[2]*Department of Genetic Engineering, Sungkyunkwan University, Suwon, Korea*
[3]*Department of Pathology, Kwandong University College of Medicine Myongji Hospital, Goyang, Korea*
[4]*Department of Palliative Medicine, Kangnam St Mary's Hospital, Catholic University, Seoul, Korea*

ABSTRACT

Tumor cells have an invasive and metastatic phenotype that is the main cause of death for cancer patients. Tumor establishment and penetration consists of a series of complex processes involving multiple changes in gene expression. In this study, intraperitoneal administration of a high concentration of ascorbic acid inhibited tumor establishment and increased survival of BALB/C mice implanted with S-180 sarcoma cancer cells. To identify proteins involved in the ascorbic acid-mediated inhibition of tumor progression, changes in the liver proteome associated with ascorbic acid treatment of BALB/C mice implanted with S-180 were investigated using two-dimensional gel electrophoresis and mass spectrometry. Eleven protein spots were identified whose expression was different between control and ascorbic acid treatment groups. In particular, Raf kinase inhibitory protein (RKIP) and annexin A5 expression were quantitatively up-regulated. The increase in RKIP protein level was detected in the tumor tissue and accompanied by an increase in mRNA level. Our results suggest a possibility that these proteins are related to the ascorbic acid-mediated suppression of tumor formation. J. Cell. Biochem. 106: 1136–1145, 2009.

KEY WORDS: RAF KINASE INHIBITORY PROTEIN; ASCORBIC ACID; PROTEOMICS

Ascorbic acid (also termed ascorbate) is toxic to cancer cells when given intravenously at high concentrations [Padayatty et al., 2004]. Increasing evidence also indicates that ascorbic acid is selectively toxic to some types of tumor cells as a pro-oxidant, rather than as an anti-oxidant [Bram et al., 1980; Bruchelt et al., 1993]. At concentrations of 10 nM–1 mM, ascorbic acid induces apoptosis in neuroblastoma and melanoma cells [Fujinaga et al., 1994; De Laurenzi et al., 1995]. Furthermore, ascorbic acid modulates mouse myeloma cell growth in vitro, as well as modulating leukemic progenitor cell growth in cells from patients with acute myeloid leukemia (AML) and myelodysplastic syndrome (MDS) [Park, 1985; Park et al., 1992, 2004].

The common characteristics of cancer cells are invasion and metastasis, both of which play important roles in secondary tumor development and progression, and which influence patient mortality. Attachment and penetration of cancer cells affects the extent of invasion and metastasis [Fidler, 1999]. Cancer cells form tumors and spread by degrading the extracellular matrix (ECM) through various matrix metalloproteinases (MMPs) [Mignatti and Rifkin, 1993]. Nutrients such as lysine and ascorbic acid are postulated to act as natural inhibitors of ECM proteolysis, and as such have the potential to inhibit tumor growth and expansion [Rath and Pauling, 1992]. These nutrients may exert their antitumor effects via inhibition of MMPs and strengthening the connective tissue surrounding cancer cells (a "tumor encapsulating" effect). Additionally, it has been suggested that, through inhibition of hyaluronidase, ascorbic acid can prevent metastases by preventing degradation of the ground substance surrounding the tumor [Roomi et al., 2005]. Different

Additional Supporting Information may be found in the online version of this article.

*Correspondence to: Dr. Seyeon Park, PhD, Department of Applied Chemistry, Dongduk Women's University, 23-1 Wolgok-dong, Sungbuk-ku, Seoul 136-714, Korea. E-mail: sypark21@dongduk.ac.kr
**Correspondence to: Chang-Hwan Yeom, Department of Palliative Medicine, Kangnam St Mary's Hospital, Catholic University, Seoul, Korea. E-mail: chyeom@cu.ac.kr

Received 19 November 2008; Accepted 14 January 2009 • DOI 10.1002/jcb.22097 • 2009 Wiley-Liss, Inc.
Published online 17 February 2009 in Wiley InterScience (www.interscience.wiley.com)

mechanisms are involved in the metastatic cascade including angiogenesis, cellular adhesion, local proteolysis, and tumor cell migration [Kohn, 1993; Fidler, 1999]. Tumor development and progression consist of a series of complex processes involving multiple changes in gene expression [Mignatti and Rifkin, 1993].

The results of several experimental studies have shown that ascorbic acid inhibits tumor growth and metastasis [Wybieralska et al., 2008]. Time-lapse analyses of Walker 256 carcinosarcoma cell migration showed that both the speed of movement and cell displacement are inhibited by ascorbic acid [Wybieralska et al., 2008]. These results demonstrate that intact, unmodified ascorbic acid applied in physiologically relevant and nontoxic concentrations exerts an inhibitory effect on the migration of WC 256 carcinosarcoma cells, and that this may be one of the factors responsible for the anti-metastatic activity of ascorbic acid. Additionally, sodium ascorbate supplementation of drinking water inhibits subcutaneous tumor growth, enhanced levodopa methylester chemotherapy, and increased survival of B 16 melanoma-bearing mice [Meadows et al., 1991]. Spontaneous metastasis was found to be inhibited by ascorbate in mice fed the restricted diet [Meadows et al., 1991]. Recently, the ability of orally administered vitamins C and K3 to inhibit the development of metastases of mouse liver tumor (TLT) cells that have been implanted into the thigh of C3H mice was evaluated [Taper et al., 2004].

We have observed that the rates of tumor formation decrease and the survival rates of the mice for 30 days increase after administration of high doses of ascorbic acid to mice implanted with S-180 cancer cells. To understand the molecular basis of ascorbic acid effect on tumor formation, we investigated the expression of proteins whose expression was altered in the presence of ascorbic acid. There has been no information on the protein products produced in tissues exposed to ascorbic acid, although numerous studies have examined the anti-cancer effect of ascorbic acid. In the present study, we performed two-dimensional gel electrophoresis (2-DE) using liver tissues of mice implanted with S-180 cancer cells following the administration of a high dose of ascorbic acid.

MATERIALS AND METHODS

MICE GROUPS

Six-week-old BALB/C mice purchased from Dae Han BioLink (Seoul, Korea) were fed a basal diet for experimental animals. The mice were assigned to one of five groups (A–E) based on the ascorbic acid administration regimen applied (Table I). Groups A and B were controls that lacked or received ascorbic acid, respectively. Group C, D, and E mice were injected with tumor cells, with subsequent injection of normal saline (group C) or ascorbic acid (group D). Mice in group E additionally received ascorbic acid before implantation of the cancer cells.

IMPLANTATION OF CANCER CELLS AND ASSESSMENT OF TUMOR FORMATION

Viable neoplastic S-180 sarcoma cells (10^6) were implanted in mice via intraperitoneal injection. S-180 cell line was a mouse cell line originated from Swiss Webster Sarcoma180 tissue. The cells were cultured in vitro in RPMI 1640 medium (Gibco, Grand Island, NY) supplemented with 10% heat-inactivated fetal bovine serum (Hyclone, Salt Lake City), 100 IU/ml penicillin, and 100 μg/ml streptomycin. The cells were subcultured at a split ratio (1:4) for injection; >95% of the total cells populations were viable as determined by the exclusion of trypan blue. The tumor formation rate was calculated according to the percent of the mice injected presenting with tumors. Mice in groups B, D, and E were intraperitoneally injected with ascorbate (1.5 mg/g body weight) every 3 days. The injections were performed by Huons Co. (Seoul, Korea). Body diameters were measured every 5 days once tumors were palpable. All mice were sacrificed by general anesthesia when spontaneous mortality appeared 30 days after tumor transplantation. The 30-day survival rate was determined for each group. For group C, D, and E mice, this survival rate represented surviving mice out of those in whom tumors had become established.

After sacrifice, a detailed general autopsy of each mouse was performed to identify tumor formation. Primary tumors and organs or tissues suspected of harboring tumor such as liver and kidneys were macroscopically examined. Samples of liver hepatocytes and kidneys were taken for detailed histological examination. These samples were fixed in 10% neutral formalin, embedded in paraffin, cut into 5–7 μm thick sections using a microtome, and stained with hematoxylin and eosin.

PREPARATION OF TOTAL PROTEIN EXTRACTS

To obtain total protein extracts, liver tissue was homogenized in 2-DE sample buffer containing 7 M urea, 2 M thiourea, 4% (w/v) CHAPS, 100 mM dithiothreitol (DTT), and a protease inhibitor cocktail (Roche, Basel, Switzerland). Tissue was disrupted by five strokes with a sonicator. After 30 min incubation with DNase (100 U/ml) at 4°C, tissue lysates were centrifuged at 45,000 rpm for 45 min at 4°C. The supernatant was collected in a new tube.

PROTEIN PURIFICATION

Precipitation using trichloroacetic acid (TCA; Sigma–Aldrich, St. Louis, MO) and acetone was performed to purify protein. TCA (50% v/v) was added to produce a final concentration of 5–8%. The sample was mixed by inversion and incubated on ice for 2 h. Following centrifugation at 14,000 rpm for 20 min the supernatant was discarded and the protein pellet was resuspended in 200 μl cold acetone. After incubation on ice for 15 min, the sample was centrifuged at 14,000 rpm for 20 min and dried. The dried pellet was dissolved in 2-DE sample buffer and the protein concentration was determined using a Bradford protein assay kit (Bio-Rad, Hercules, CA).

ISOELECTRIC FOCUSING (IEF)

Protein (800 μg) was diluted to a final volume of 300 μl in sample buffer containing 7 M urea, 2 M thiourea, 4% (w/v) CHAPS, 100 mM DTT, and 0.5% carrier ampholyte (pH 4–7, Bio-Rad) and loaded on a 17 cm long gel with pH 4–7 gradient. A rehydrated immobilized pH gradient (IPG) strip was positioned gel side-down on the strip tray and covered with mineral oil. The voltage was sequentially increased from 100–8,000 V to attain 80,000 total voltage h (300 Vh at 100 V, 400 Vh at 200 V, 1,000 Vh at 500 V, 1,000 Vh at 1,000 V, 2,000 Vh at 2,000 V, 4,000 Vh at 4,000 V, for a total of 80,000 Vh at 8,000 V). During IEF, the temperature was set to 20°C. To solubilize the

focused proteins, the IPGs were soaked in sodium dodecyl sulfate (SDS) equilibration buffer containing 6 M urea, 2% (w/v) SDS, 0.05 M Tris–HCl (pH 8.8), and 20% glycerol. The strip was treated with 10 ml of an equilibration solution containing 6 M urea, 2% (w/v) SDS, 0.05 M Tris–HCl (pH 8.8), 20% glycerol, and 20% DTT, and placed on a shaker for 10 min. Then strip was shaken in 10 ml of iodoacetamide (IAA) equilibration solution containing 6 M urea, 2%(w/v) SDS, 0.05 M Tris–HCl (pH 8.8), 20% glycerol, and 25% IAA for another 10 min. After briefly rinsing with 1× gel buffer, the IPG strip was loaded on the top of 12% SDS–polyacrylamide gel electrophoresis (PAGE) gel. Low melting point agarose consisting of 1% molten agarose solution with a trace amount of bromophenol blue was added. SDS–PAGE was performed for 30 min at a constant current of 16 mA and then at 24 mA at 4°C.

2-DE GEL IMAGE ANALYSIS

Electrophoretically separated proteins were visualized by Coomassie brilliant blue G-250 staining of the gels. Images were digitalized using a GS-800 calibrated densitometer (Bio-Rad) and analyzed by PD Quest 2-D software (Bio-Rad). Quantitative differences were determined only when a matched spot displayed the same degree of down- or up-regulation in duplicate experiments. Matching spots in gels from the same sample were identified and their intensities were measured using an Image Master 2-D system. Analysis was performed on approximate 170 different protein spots per sample. For each spot, the intensity value obtained in the ascorbic acid-treated gel was divided by that obtained in the control gel. The logs of these ratios (LR; the means and median values clustered around the 0 value) were then calculated. LR was expected if errors were associated with the analysis were random and normally distributed. Spots showing an expression 3.0-fold less or greater than the control were considered to represent a statistically significant differentially expressed protein species.

IN-GEL ENZYMATIC DIGESTION AND MASS SPECTROMETRY

Spots were excised from the stained gel, destained with 50 mM ammonium bicarbonate in 40% acetonitrile, and dried with a Speed Vac plus SC1 10 (Savant Holbook, HY). The excised spot was rehydrated in 10 ng/μl trypsin in 50 mM ammonium bicarbonate. After the rehydrated spot was placed on ice for 45 min and treated with 50 mM ammonium bicarbonate (10 μl), it was incubated at 37°C for 12 h.

MATRIX ASSISTED LASER-DESORPTION IONIZATION TIME-OF-FLIGHT TANDEM MASS SPECTROSCOPY (MALDI TOF-MS/MS)

Digested samples were removed and subjected to a desalting/concentration step on a mZipTipC18 column (Millipore, Billerica, MA) using acetonitrile as an eluent before MALDI-TOF-MS/MS analysis. Peptide mixtures were loaded on the MALDI system using the dried-droplet technique and α-cyano-4-hydroxycinnamic acid (Sigma) as matrix, and were analyzed using a 4700 Reflector spec #1 mass spectrometer (Applied Biosystems, Framingham, MA). Internal mass calibration was performed using peptides derived from enzyme autoproteolysis. The Data explorer software package (Applied Biosystems) was used to identify spots from the ProFound database by mass searching all taxa sequences. Candidates identified by peptide mapping analysis were evaluated further by comparing their calculated masses and isoelectric points using the experimental values obtained by 2-DE.

WESTERN-BLOT ANALYSIS

To determine the expression level of Raf kinase inhibitory protein (RKIP) and annexin A5, protein extracts were obtained from liver tissue treated or untreated with ascorbic acid and analyzed by 12% SDS–PAGE. The separated proteins were transferred to a nitrocellulose membrane (Schleicher and Schuell, Keene, NH). After transfer, the membrane was saturated by incubation, at 4°C overnight with 5% (w/v) non-fat dry milk in Tris-buffered saline (TBS)—01% Tween-20 (TBST) and then incubated with RKIP antibody (Becton and Dickinson Biosciences, San Jose, CA) for 3 h. After washing with TBST, the membrane was incubated with an anti-rabbit immunoglobulin coupled with peroxidase (Santa Cruz Biotechnology, Santa Cruz, CA). After 60 min of incubation at room temperature, the membrane was washed three times with TBST and the blots were developed using enhanced chemiluminescence (ECL1; Amersham Biosciences, Buckinghamshire, UK). Normalization was performed using polyclonal β-actin antibody (Santa Cruz Biotechnology). Blots were quantified using a Gel Doc 2000 densitometer (Bio-Rad).

RNA ISOLATION AND POLYMERASE CHAIN REACTION (PCR)

PCR was performed to validate the protein expression level. Total RNA was extracted by homogenization in Trizol reagent (Invitrogen, Carlsbad, CA) according to the manufacturer's instructions from both the liver and isolated tumor tissue of each mouse. Synthesis of cDNA was performed as previously described [Yang et al., 2003]. Briefly, 50 μg of total RNA was reverse-transcribed to double stranded cDNA using an oligo-dT primer. For PCR analysis, primer pairs were designed for *RKIP*. The information for each probe was obtained from the Stanford Online Universal Resource for Clones and ESTs (SOURCE; http://www.source.stanford.edu), which compiles information from several publicly accessible databases including UniGene, dbEST, Swiss-Prot, GeneMap99, RHdb, GeneCards, and LocusLink. Each probe was designed to yield a 175 bp amplicon and to have a melting temperature of about 60°C. Normalization was performed using a glyceraldehyde-3-phosphate dehydrogenase (GAPDH) primer. PCR (20 cycles) was performed using Taq polymerase (Qiagen, Valencia, CA) and oligonucleotide primers for mouse RKIP (forward: 5′-GGATAGTCCCATCCCAGGTT-3′, reverse: 5′-ACCACTCACAGACACCACCA-3′, amplicon size 175 bp) and GAPDH (forward: 5′-AACTTTGGCATTGTGGAAGG-3′, reverse: 5′-AGTTGTCATTGAGAGCAATG-3′, amplicon size 421 bp). PCR products were analyzed by fractionation on a 1.2% agarose gel and visualized by ethidium bromide staining. Images were captured using the Quantity One gel documentation system (Bio-Rad).

RESULTS

INFLUENCE OF ASCORBATE ON TUMOR FORMATION AND SURVIVAL

In mice injected with S-180 tumor cells, ascorbic acid treatment inhibited tumor formation during the treatment period (Fig. 1A). The

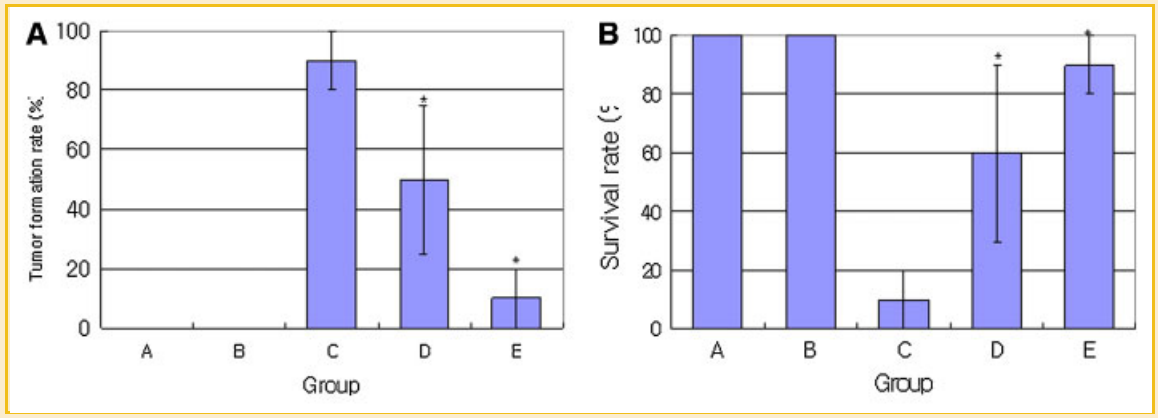

Fig. 1. Effect of ascorbic acid on tumor formation rate (A) and survival rate (B). Thirty-day survival rate was determined within each group. In case of groups C, D, and E, the survival rate represented survival of tumor-implanted mice. The values were obtained from eight independent experiments. In each experiment, each group was composed of 10 mice. Data represent the mean ± SD. Asterisk (*) indicates $P < 0.05$ compared to control group C (Student's t test). [Color figure can be viewed in the online issue, which is available at www.interscience.wiley.com.]

tumor then began to grow and caused ascites. Survival of mice sensitive to ascorbate (groups D and E) was more than twice that of the survival of mice in group C (Fig. 1B). Due to ascites, the mean body width of group C mice was larger than that of ascorbate-treated mice in groups D and E (Fig. 2 and supplementary data). Soon after tumor injection, ascorbic acid treatment produced a distinct inhibition of solidification and ascites. Mortality was accelerated by tumor necrosis, ulcerations, and infections. Histological examinations were performed on some of the dead mice. The examined primary tumors were voluminous and often exhibited large ulcerations and subsequent dissemination of their contents with macroscopically detectable metastases.

We next investigated whether there was any difference in tumor metastases between the control and experimental groups of mice. Macroscopic and microscopic examinations of serial liver sections revealed a distinct difference in the number of mice bearing liver

TABLE I. Mice Groups* Based on Ascorbic Acid Administration

Days	Group A	Group B	Group C	Group D	Group E
0	NT	LAA	NT	NT	LAA
2	NT	LAA	NT	NT	LAA
4	NT	LAA	NT	NT	LAA
6	NT	LAA	NT	NT	LAA
8	NT	LAA	NT	NT	LAA
10	NT	LAA	S-180	S-180	S-180
12	NT	LAA	NT	LAA	LAA
14	NT	LAA	NT	LAA	LAA
16	NT	LAA	NT	LAA	LAA
18	NT	LAA	NT	LAA	LAA
20	NT	LAA	NT	LAA	LAA
22	NT	LAA	NT	LAA	LAA
24	NT	LAA	NT	LAA	LAA
26	NT	LAA	NT	LAA	LAA
28	NT	LAA	NT	LAA	LAA
30	NT	LAA	NT	LAA	LAA

*In each experiment each group was composed of 10 mice.

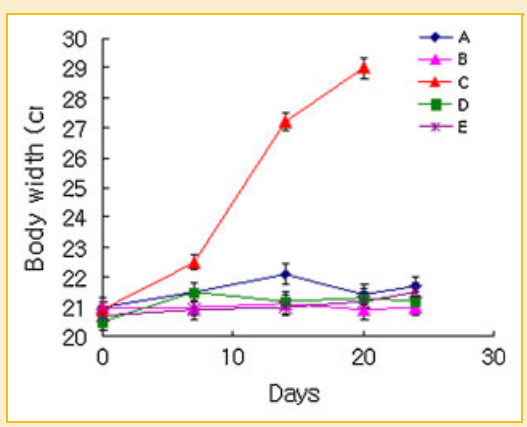

Fig. 2. Effect of ascorbic acid on tumorigenic ascites. Body diameters were measured every 5 days once tumors were palpable. The values are obtained from eight independent experiments. In each experiment, each group was composed of 10 mice. Data represent the mean ± SD. [Color figure can be viewed in the online issue, which is available at www.interscience.wiley.com.]

metastases between the control and the ascorbic acid-treated groups of mice. Detailed autopsies and microscopic examinations (Fig. 3) showed metastases in the hepatocytes, which displayed an eosinophilic cytoplasm with round nuclei. These were contained within in the liver hepatocytes rather than being present on the stroma of the liver. In the experimental group, seven of 31 mice (23%) exhibited liver metastases, while 12 of 30 control mice (40%) possessed liver metastases (Table II), showing a distinct and significant ($P = 0.034$) reduction in the ascorbic acid-treated group as compared with the control group. Detailed autopsies and microscopic examinations (Fig. 3) did not demonstrate metastases in any kidney.

CHANGES IN LIVER TISSUE PROTEOME PROFILE AFTER ASCORBIC ACID TREATMENT

To investigate the alterations associated with liver metastasis on a molecular basis, proteomic differential display analysis for the expression of proteins in the liver tissue of mice in groups C, D, and E was performed by 2-D gel electrophoresis and MALDI-TOF MS/MS. Protein expression was assessed in six samples each from each group

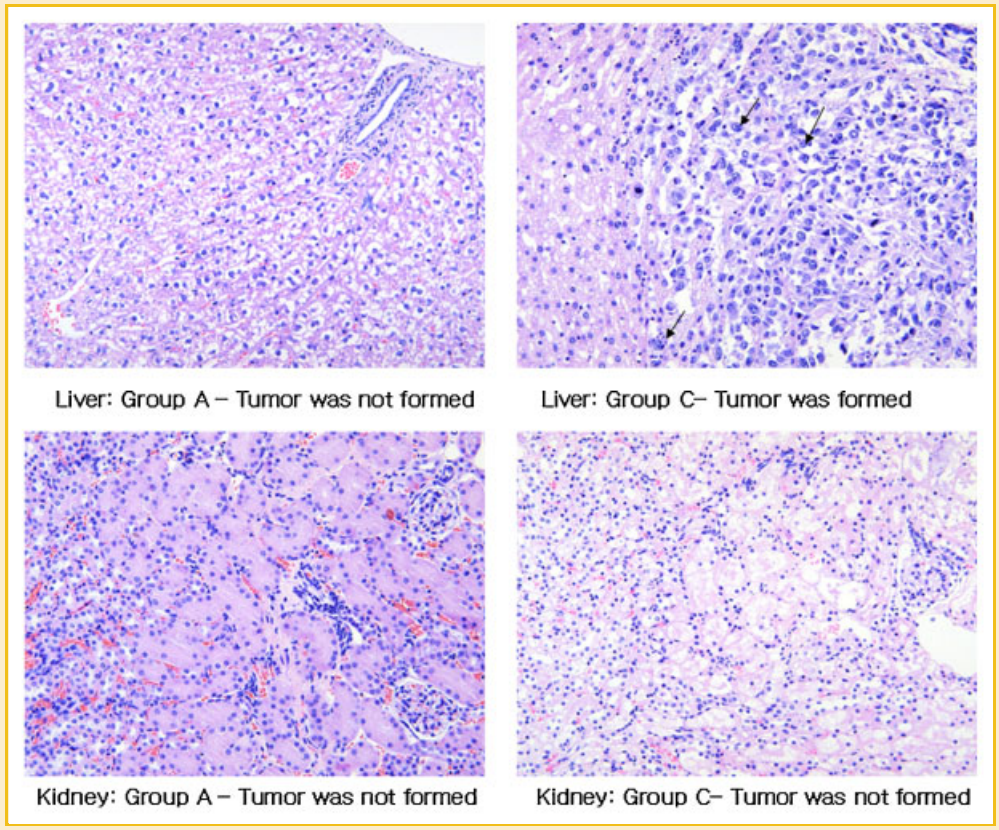

Fig. 3. Histological aspects of carcinoma cells in liver tissue of a group C mouse. The magnification views (200×) of group C cells shows cell pleiomorphism and several multi nuclei (arrows) in the tumor. Throughout the fields of view, nuclei display large to enormous oblong nucleoli. [Color figure can be viewed in the online issue, which is available at www.interscience.wiley.com.]

obtained on the same schedule under the same conditions. To investigate the liver proteome changes, mice with macroscopically and microscopically visible metastases in the liver tissue were analyzed. More than 150 protein spots were visualized on the 2-DE gels, and the differences in spot intensities between groups C and D or between groups C and E were compared visually and analyzed for each gel. Expression comparisons of each Coomassie brilliant blue-stained spot are shown in Figure 4. Eleven protein spots whose expression differed between groups C and E were apparent. Of these, the expression of eight proteins was associated with the presence of ascorbic acid, with significant differences ($P < 0.05$); six proteins were over-expressed and two proteins were down-regulated (Table III). Additionally, 18 protein spots whose expression differed between groups C and D were evident; of these, 11 proteins were over-expressed and one protein was down-regulated after ascorbic acid treatment with significant differences ($P < 0.05$) (Table III). The volume of two protein spots changed significantly ($P < 0.01$, Student's *t*-test) (Fig. 5). These two proteins were identified as RKIP (Accession number AAG25635.1) and annexin A5 (ANXA5, Accession number AAH03716.1).

TABLE II. Effects of Ascorbic Acid on the Incidence of Liver Tumor Formation in BALB/C Mice Transplanted With S-180

Group	Number of mice with liver tumor per total mice	% mice with liver tumor
C	12/30	40%
D	7/31	23%

*A two-tailed t-distribution test was used for statistical analysis of results ($P = 0.034$).

VERIFICATION OF DIFFERENTIALLY EXPRESSED PROTEINS

From the identified candidates, RKIP was detected by Western blot analysis (Fig. 6A). The expression changes of this protein were consistent with 2-DE results. To test the tissue-specificity of ascorbic acid-induced expression of RKIP, RKIP levels in kidney tissue were also examined. RKIP was up-regulated in liver tissue and the kidney of ascorbic acid-treated mice in groups D and E compared with group C mice. RKIP is known to inhibit Raf 1-mediated phosphorylation of MAPK/ERK kinase (MEK) through binding to Raf 1 [Yeung et al., 1999]. To validate the up-regulation of RKIP functionally, MEK phosphorylation was investigated. As shown in Figure 6B, the level of MEK phosphorylation was significantly decreased ($P < 0.01$) in both liver and kidney tissues of ascorbic acid-treated mice compared with group C control tissues. To test the tumor tissue-specificity of ascorbic acid-induced expression of RKIP, RKIP levels in tumor tissue were compared between groups C

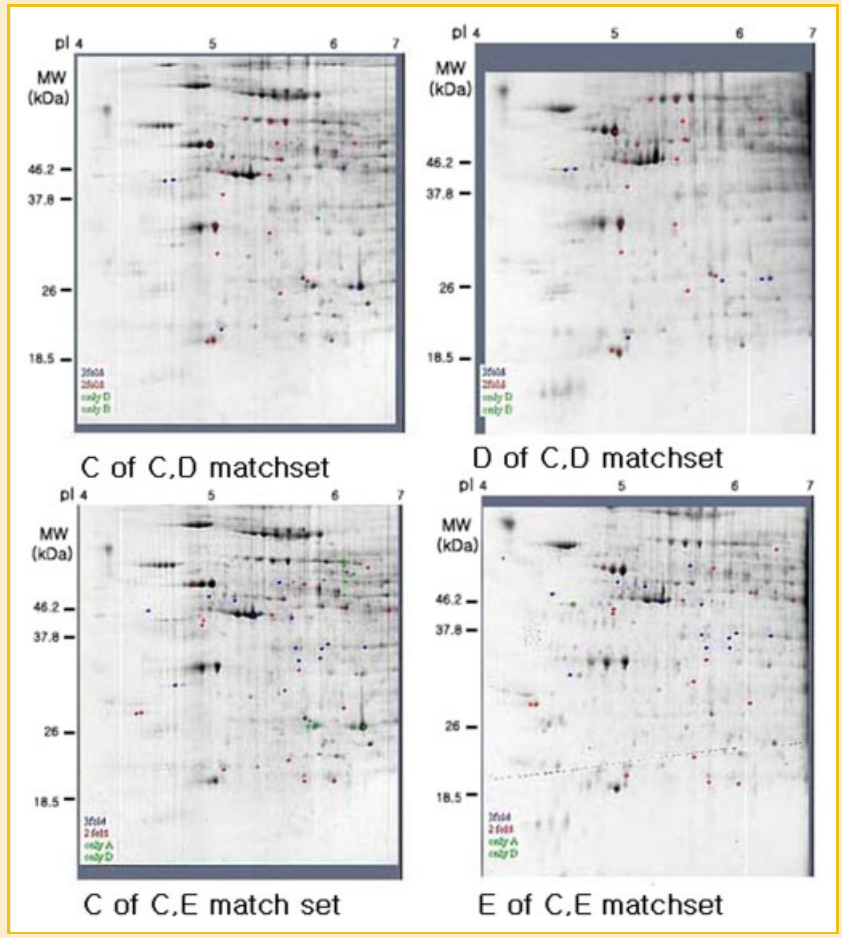

Fig. 4. Examination of liver proteins by 2-DE. Results shown are representative of four independent experiments. The images were analyzed by ImageMaster 2D software and proteins were identified by MALDI-TOF MS/MS. Total protein extracts were analyzed by 2-DE and gels were stained with Coomassie brilliant blue G-250. Vertical axes represent apparent molecular mass (kDa) and horizontal axes pH values. Acquired images of four independent experiments showed repetitive pattern. [Color figure can be viewed in the online issue, which is available at www.interscience.wiley.com.]

and D. Western blot analysis revealed that there were marked differences in RKIP expression between two groups (Fig. 6). The rate of tumor formation in group E was low, which made it difficult to analyze the difference of RKIP expression between the tumors in groups C and E.

The expression changes of ANXA5 protein were also consistent with 2-DE results as shown in Figure 7. ANXA5 was up-regulated in liver and tumor tissues of ascorbic acid-treated mice in group D compared with group C mice.

ASCORBIC ACID-INDUCED EXPRESSION OF RKIP PROTEIN AND mRNA

To investigate whether there was a relationship between RKIP protein levels and expression of this protein, the mRNA level was measured using reverse transcription-PCR analysis of RKIP expression. As shown in Figure 8, RKIP mRNA levels were significantly increased in liver and tumor tissue in ascorbic acid treatment group (Liver, $P_{CE} < 0.01$; Tumor, $P_{CD} < 0.01$).

DISCUSSION

Presently, we demonstrate that a high concentration of ascorbic acid supplementation increases the survival rate of mice bearing intraperitoneal injected S-180 sarcoma cells, and that the administration of ascorbic acid inhibits tumor development. Detailed microscopic examination of the liver revealed an inhibitory effect of ascorbic acid treatment on the development of metastases. As was the case in previous studies [Taper et al., 2004], oral administration of vitamins C and K3 produced a distinct inhibitory effect on the development of metastases in C3H mice bearing an intramuscularly transplanted mouse liver tumor. Detailed microscopic examination of the main organs as well as the lungs and local lymph nodes (other tissues known to harbor metastases from this tumor) have revealed a distinct inhibitory effect of oral vitamin treatment on the development of metastases [Taper et al., 2004]. Also, ascorbate supplementation augments the growth-inhibitory effect of dietary tyrosine and phenylalanine restriction on both primary and metastatic tumor growth indicating an important adjuvant role

TABLE III. Protein Spots Altered Between Groups C and D, and Between Groups C and E

Spot between	Protein description[a]	Measured Mr (kDa)/PI	Intensity variation[b]	MALDI-TOF coverage (%)[c]
CE1	Succinate-coenzyme A ligase, GDP-forming, β subunit	47.09/6.6	Ur (4.41 ± 1.29)	33
CE3	Annexin A5	35.78/4.8	Ur (4.15 ± 0.18)*	37
CE4	Heat-shock protein hsp84	83.56/4.9	Ur (4.09 ± 1.13)	15
CE5	Ribosomal protein SA	33.01/4.8	Ur (6.30 ± 2.01)	40
CE6	Fructose bisphosphatase 1	37.29/6.2	Ur (4.86 ± 1.19)	45
CE7	Eukaryotic translation initiation factor 3, subunit 2 (beta)	36.84/5.4	Ur (3.91 ± 0.79)	26
CE9	Purine nucleoside phosphorylase	32.54/5.9	Dr (0.314 ± 0.012)	27
CE10	Chain A, recombinant mouse L-chain ferritin	20.68/5.6	Dr (0.224 ± 0.064)	60
CD4	Galactokinase	42.68/5.2	Ur (5.56 ± 2.17)	28
CD5	Pyrophosphatase	33.11/5.4	Ur (3.34 ± 0.22)	45
CD6	Guanidinoacetate methyltransferase	26.6/5.4	Ur (4.27 ± 1.09)	51
CD7	MAWD binding protein homolog 2	32.19/5.2	Ur (5.28 ± 2.04)	32
CD9	Raf kinase inhibitory protein (RKIP) phosphatidylethanolamine-binding protein 1 (PEBP1)	20.98/5.2	Ur (8.60 ± 1.06)*	66
CD10	Lactoylglutathione lyase	20.90/5.2	Ur (4.54 ± 1.28)	32
CD11	Epsilon isoform of 14-3-3 protein	29.33/4.6	Ur (5.74 ± 2.10)	22
CD13	Annexin A5	35.78/4.8	Ur (4.79 ± 0.64)*	z53
CD14	GTP-specific succinyl-CoA synthetase β subunit	40.44/5.2	Ur (4.11 ± 0.98)	45
CD16	Guanidinoacetate methyltransferase	26.6/5.4	Ur (4.36 ± 1.18)	57
CD17	Purine nucleoside phosphorylase	32.54/5.8	Dr (0.251 ± 0.043)	58
CD19	NADH dehydrogenase (ubiquinone) Fe-S protein 3	30.36/6.4	Ur (4.41 ± 1.36)	38

Asterisk (*) indicates the significant difference between spots by student's t test ($P < 0.01$), (Ur, up-regulated; Dr, down-regulated).
[a]List of spots/proteins sensitive to ascorbic acid treatment in mice groups, detected by 2-DE and identified by peptide mass fingerprint analysis based on the ProFound database searched using the Data Explorer program.
[b]Intensity variation is represented as the mean ± SD of each spot. The intensity of the each spot was calculated by single spot normalization using the image Master 2-D system.
[c]Peptide coverage represents the percentage of matching sequences (Mr, molecular weight; PI, isoelectric point).

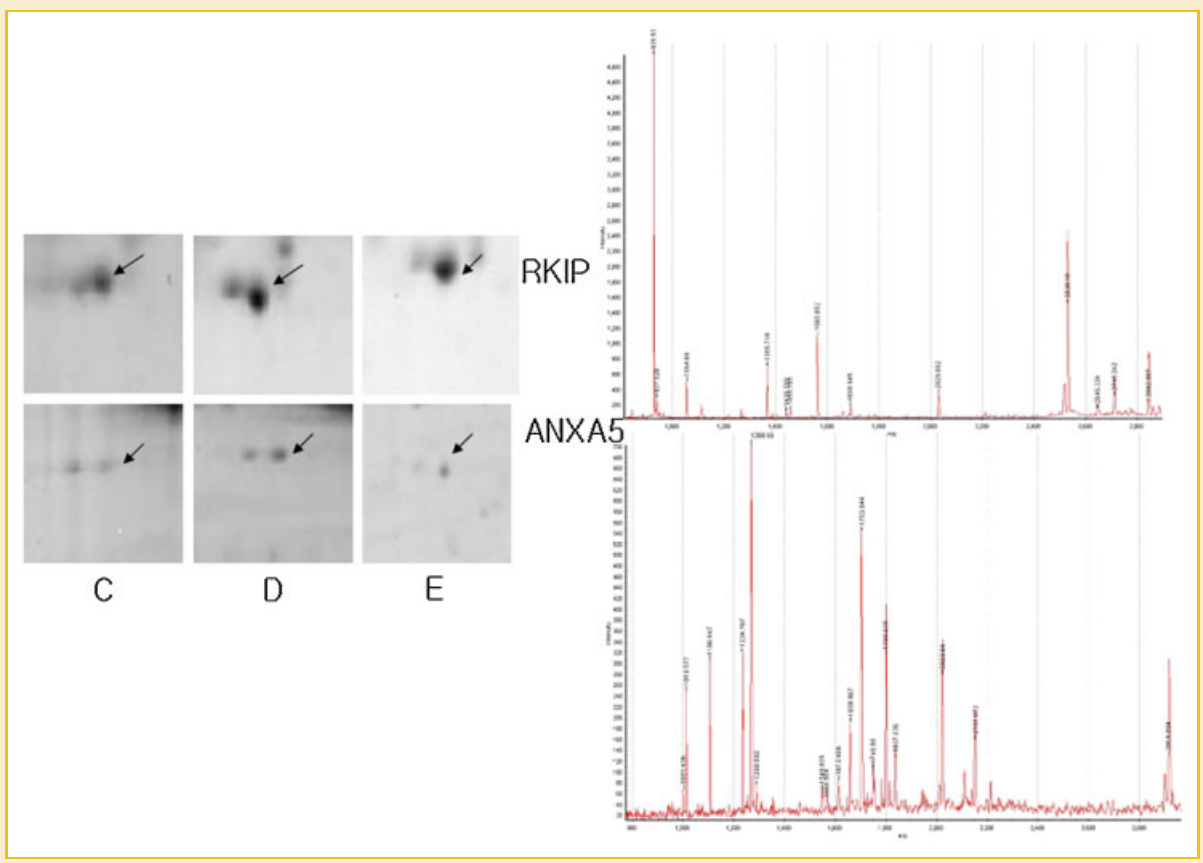

Fig. 5. Spots and spectra from MALDI-TOF MS/MS analysis of the trypsin digestion product of RKIP and ANXA5. Peptide mixtures were loaded on the MALDI system, using the dried-droplet technique and α-cyano-4-hydroxycinnamic acid as matrix, and were analyzed using a 4700 Reflector spec #1 mass spectrometer. MALDI-TOF coverage was 66% for RKIP and 53% for ANXA5. [Color figure can be viewed in the online issue, which is available at www.interscience.wiley.com.]

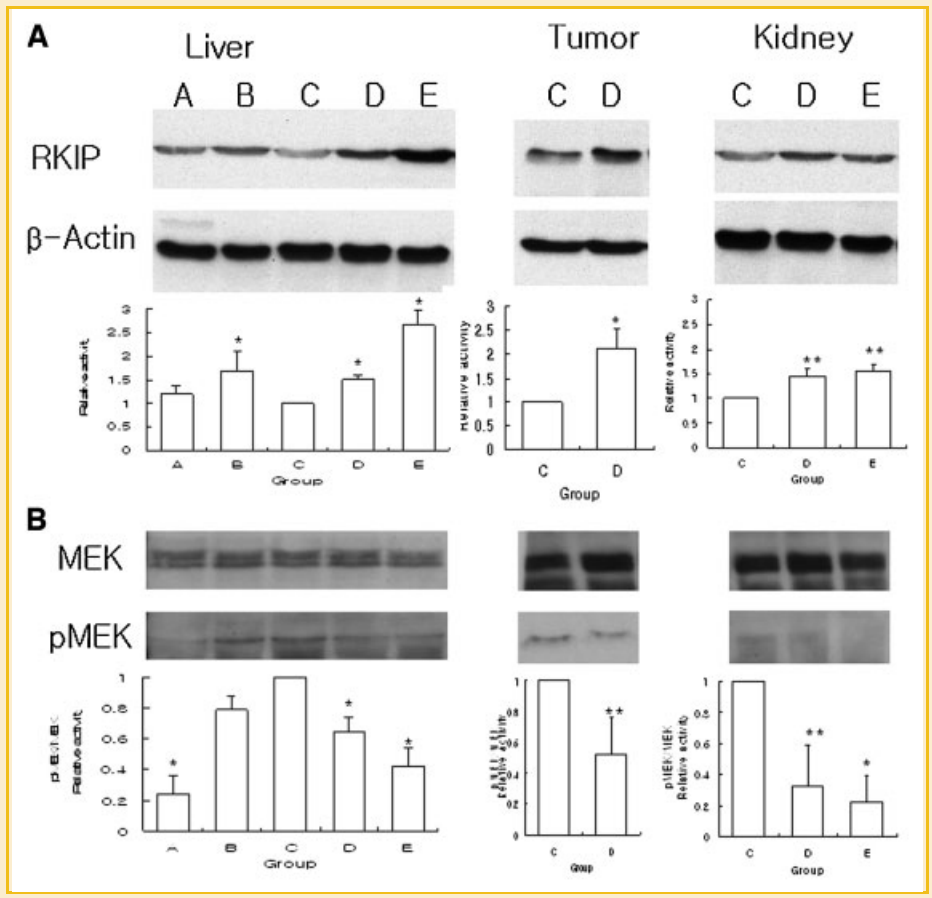

Fig. 6. Western blot analyses. A: Western blot of RKIP levels in liver, kidney, and tumor tissues. RKIP levels were elevated in ascorbic acid-treated mice. RKIP levels for each group were normalized to β-actin level. Similar results were obtained with 2-DE. Each data point represents a mean of three individual values and standard deviations. Quantitative analysis was performed using student's *t* test and results are expressed as relative activity to untreated control group C. Asterisks indicate statistically significant difference between treatment and untreated control condition ($^{*}P < 0.01$, $^{**}P < 0.05$). B: Western blot analysis of MEK phosphorylation levels in liver, kidney, and tumor tissues. MEK phosphorylation levels were lowered in ascorbic acid-treated mice. Phosphorylation levels for each group were normalized to MEK level and are presented as the normalized ratio to that of group C. Each data point represents a mean of three individual values and standard deviations. Asterisks indicate statistically significant difference between treatment and untreated control condition ($^{*}P < 0.01$, $^{**}P < 0.05$).

[Meadows et al., 1991]. Similarly, in Ehrlich ascites tumors ascorbate reduces invasion and the tumors are characterized by long regions of basement membrane in the connective-tissue stroma [Gruber et al., 1980].

The mechanism of the action of ascorbic acid on tumor establishment and metastases is unknown. The aim of the present study was to identify molecular changes coincident with susceptibility to ascorbic acid. The proteomic approach was employed to screen a number of proteins that were differentially regulated by ascorbic acid treatment. Among the implicated proteins were metabolic proteins including succinate-coenzyme A ligase, fructose bisphosphatase 1, galactokinase, pyrophosphatase, guanidinoacetate methyltransferase, lactoylglutathione lyase, GTP-specific succinyl-CoA synthetase β subunit, and NADH dehydrogenase. RKIP protein was intensified in group D compared to group C and ANXA5 was intensified in group D and E compared to group C.

RKIP is a phosphatidylethanolamine binding protein (PEBP) [Bernier et al., 1986], first documented as an important regulator of the mitogen activated protein kinase (MAPK) signal transduction pathway, whose role is to rapidly convert extracellular signals into activation of transcription factors [Chang and Karin, 2001; Pearson et al., 2001; Kondoh et al., 2005; Trakul and Rosner, 2005]. To date, RKIP-1 is the only known cellular inhibitor of Raf kinase. Other signaling pathways are also influenced by RKIP-1. For example, the inhibition of RKIP-1 enhances NF-κB-induced transcription while over-expression reduces this transcription [Yeung et al., 2001]. In addition, RKIP-1 impinges on G-protein coupled receptor signaling by controlling the activity of the G-protein coupled receptor kinase-2 [Kroslak et al., 2001; Lorenz et al., 2003]. The functions of RKIP-1 in a variety of organisms are diverse and include inhibition of carboxypeptidase Y in yeast [Bruun et al., 1998], an immunoprotective function in nematodes [Frayne et al., 1999], odorant binding and detection in Drosophila [Frayne et al., 1999], and control of shoot growth and flowering in plants [Pnueli et al., 2001]. In mammals, signaling proteins are often linked to disease states [Krupnick and Benovic, 1998], and recent work indicates that

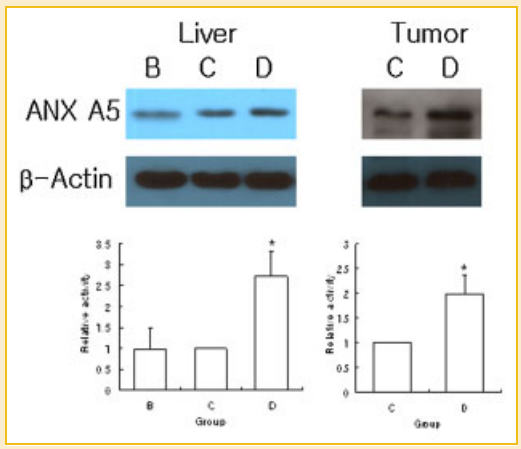

Fig. 7. Western blot of annexin A5 levels in liver and tumor tissues. ANXA5 levels were elevated in ascorbic acid-treated mice. ANXA5 levels for each group were normalized to β-actin level. Similar results were obtained with 2-DE. Each data point represents a mean of three individual values and standard deviations. Quantitative analysis was performed using Student's *t* test and results are expressed as relative activity to untreated control group C. Asterisks indicate statistically significant difference between treatment and untreated control condition ($^*P < 0.01$). [Color figure can be viewed in the online issue, which is available at www.interscience.wiley.com.]

RKIP-1 is a metastasis suppressor [Fu et al., 2003; Chatterjee et al., 2004; Keller et al., 2005; Park et al., 2005]. RKIP is not a substrate for Raf-1 or MEK but it appears that RKIP acts to set the threshold for Raf-1 activation and subsequent activation of the MEK/ERK pathway [Keller et al., 2004]. Raf-1 dissociates from its complex with MEK in the presence of RKIP. As a result, downstream MAPK signaling is interrupted and diminished [Keller et al., 2004]. To further assess the function of RKIP in Raf signaling, the phosphorylation of Raf substrate MEK was presently investigated.

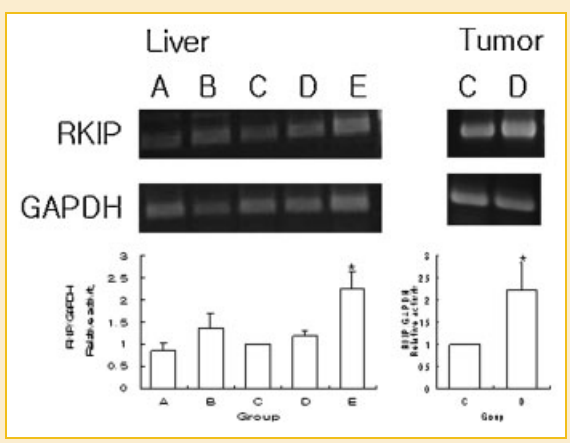

Fig. 8. RT-PCR analysis of RKIP mRNA levels in liver and tumor tissues. RKIP levels for each group were normalized to GAPDH level. Each data point represents a mean of three individual values and standard deviations. Quantitative analysis was performed and results are expressed as relative activity to untreated control group C. Asterisks indicate statistically significant difference between treatment and untreated control condition ($^*P < 0.01$).

Tissues from mice with metastatic liver tumors showed increased RKIP expression and aberrant MEK phosphorylation, consistent with the demonstration that metastatic prostate cancer cells have much less RKIP expression than non-metastatic prostate cancer cells [Keller et al., 2004].

The mechanisms through which RKIP suppresses metastasis are not known. However, the present observation that increased RKIP expression was associated with decreased tumor formation and metastasis suggests that RKIP may act at the tumor establishment stages of metastasis.

ANXA5 induces suppression of tumor metastasis [Markoff et al., 2007]. This calcium- and phospholipid-binding protein interacts with the N-terminal leucine-rich repeats of polycystin-1 both in vitro and in a cell culture model [Markoff et al., 2007]. This interaction is direct, specific, and involves a conserved sequence of the ANXA5 N-terminal domain [Markoff et al., 2007]. Using Madin-Darby canine kidney cells expressing polycystin-1 in an inducible manner, it was also shown that polycystin-1 co-localizes with E-cadherin at the cell-cell contacts, accelerating the recruitment of intracellular E-cadherin to reforming junctions. This polycystin-1-stimulated recruitment is significantly delayed by extracellular annexin A5 [Markoff et al., 2007]. Although the precise function of these proteins in tumor metastasis still remains elusive, our results suggest a possibility that these proteins may be related to the ascorbic acid-mediated suppression of tumor metastasis.

ACKNOWLEDGMENTS

This research was funded by Korean Association for Vitamin Research.

REFERENCES

Bernier I, Tresca JP, Jolles P. 1986. Ligand-binding studies with a 23 kDa protein purified from bovine brain cytosol. Biochim Biophys Acta 871:19–23.

Bram S, Froussard P, Guichard M, Jasmin C, Augery Y, Sinoussi-Barre F, Wray W. 1980. Ascorbic acid preferential toxicity for malignant melanoma cells. Nature 284:629–631.

Bruchelt G, Baader L, Reith AG, Holger NL, Gebhardt S, Niethammer D. 1993. Rationale for the use of ascorbic acid in neuroblastoma therapy. Human Neuroblastoma. Newark: Harwood Academic Publishers. pp 34–40.

Bruun AW, Svendsen I, Sorensen SO, Kielland-Brandt MC, Winther JR. 1998. A high-affinity inhibitor of yeast carboxypeptidase Y is encoded by TFS1 and shows homology to a family of lipid binding proteins. Biochemistry 37: 3351–3357.

Chang L, Karin M. 2001. Mammalian MAP kinase signalling cascades. Nature 410:37–40.

Chatterjee D, Bai Y, Wang Z, Beach S, Mott S, Roy R, Braastad C, Sun Y, Mukhopadhyay A, Aggarwal BB, Darnowski J, Pantazis P, Wyche J, Fu Z, Kitagwa Y, Keller ET, Sedivy JM, Yeung KC. 2004. RKIP sensitizes prostate and breast cancer cells to drug-induced apoptosis. J Biol Chem 279:17515–17523.

De Laurenzi V, Melino G, Savini I, Annicchiarico-Petruzzelli M, Finazzi-Agro A, Avigliano L. 1995. Cell death by oxidative stress and ascorbic acid regeneration in human neuroectodermal cell lines. Eur J Cancer 31A:463–466.

Fidler IJ. 1999. Critical determinants of cancer metastasis: Rationale for therapy. Cancer Chemother Pharmacol 43:S3–S10.

Frayne J, Ingram C, Love S, Hall H. 1999. Localisation of phosphatidylethanolamine-binding protein in the brain and other tissues of the rat. Cell Tissue Res 298:415–423.

Fu Z, Smith PC, Zhang L, Rubin MA, Dunn RL, Yao Z, Keller ET. 2003. Effects of raf kinase inhibitor protein expression on suppression of prostate cancer metastasis. J Natl Cancer Inst 95:878–889.

Fujinaga S, Sakagami H, Kuribayashi N, Takahashi H, Amano Y, Sakagami T, Takeda M. 1994. Possible role of hydrogen peroxide in apoptosis induction by ascorbic acid in human myelogenous leukemic cell lines. Showa Univ Med Sci 6:135–144.

Gruber HE, Tewfik HH, Tewfik FA. 1980. Cytoarchitecture of Ehrlich ascites carcinoma implanted in the hind limb of ascorbic acid-supplemented mice. Eur J Cancer 16:441–448.

Keller ET, Fu Z, Brennan M. 2004. The role of Raf kinase inhibitor protein (RKIP) in health and disease. Biochem Pharmacol 68:1049–1053.

Keller ET, Fu Z, Brennan M. 2005. The biology of a prostate cancer metastasis suppressor protein: Raf kinase inhibitor protein. J Cell Biochem 94:273–278.

Kohn EC. 1993. Development and prevention of metastasis. Anticancer Res 13:2553–2559.

Kondoh K, Torii S, Nishida E. 2005. Control of MAP kinase signaling to the nucleus. Chromosoma 114:86–91.

Kroslak T, Koch T, Kahl E, Hollt V. 2001. Human phosphatidylethanolaminebinding protein facilitates heterotrimeric G protein-dependent signaling. J Biol Chem 276:39772–39778.

Krupnick JG, Benovic JL. 1998. The role of receptor kinases and arrestins in G protein-coupled receptor regulation. Annu Rev Pharmacol Toxicol 38:289–319.

Lorenz K, Lohse MJ, Quitterer U. 2003. Protein kinase C switches the Raf kinase inhibitor from Raf-1 to GRK-2. Nature 426:574–579.

Markoff A, Bogdanova N, Knop M, Rüffer C, Kenis H, Lux P, Reutelingsperger C, Todorov V, Dworniczak B, Horst J, Gerke V. 2007. Annexin A5 interacts with polycystin-1 and interferes with the polycystin-1 stimulated recruitment of E-cadherin into adherens junctions. J Mol Biol 369:954–966.

Meadows GG, Pierson HF, Abdallah RM. 1991. Ascorbate in the treatment of experimental transplanted melanoma. Am J Clin Nutr 54:1284S–1291S.

Mignatti P, Rifkin DB. 1993. Biology and biochemistry of proteinases in tumor invasion. Physiol Rev 73:161–195.

Padayatty SJ, Sun H, Wang Y, Riordan HD, Hewitt SM, Katz A, Wesley RA, Levine M. 2004. Vitamin C pharmacokinetics: Implications for oral and intravenous use. Ann Intern Med 140:533–537.

Park CH. 1985. Biological nature of the effect of ascorbic acids on the growth of human leukemic cells. Cancer Res 45:3969–3973.

Park CH, Kimler BF, Bodensteiner D, Lynch SR, Hassanein RS. 1992. In vitro growth modulation by L-ascorbic acid of colony-forming cells from bone marrow of patients with myelodysplastic syndromes. Cancer Res 52:4458–4466.

Park S, Han SS, Park CH, Hahm ER, Lee SJ, Park HK, Lee SH, Kim WS, Jung CW, Park K, Riordan HD, Kimler BF, Kim K, Lee JH. 2004. L-Ascorbic acid induces apoptosis in acute myeloid leukemia cells via hydrogen peroxidemediated mechanisms. Int J Biochem Cell Biol 36:2180–2195.

Park S, Yeung ML, Beach S, Shields JM, Yeung KC. 2005. RKIP downregulates B-Raf kinase activity in melanoma cancer cells. Oncogene 24: 3535–3540.

Pearson G, Robinson F, Beers Gibson T, Xu BE, Karandikar M, Berman K, Cobb MH. 2001. Mitogen-activated protein (MAP) kinase pathways: Regulation and physiological functions. Endocr Rev 22:153–183.

Pnueli L, Gutfinger T, Hareven D, Ben-Nairn O, Ron N, Adir N, Lifschitz E. 2001. Tomato SP-interacting proteins define a conserved signaling system that regulates shoot architecture and flowering. Plant Cell 13: 2687–2702.

Rath M, Pauling L. 1992. Plasmin-induced proteolysis and the role of apoprotein(a), lysine and synthetic analogs. Orthomol Med 7:17–23.

Roomi MW, Roomi NW, Ivanov V, Kalinovsky T, Niedzwiecki A, Rath M. 2005. Modulation of N-methyl-N-nitrosourea induced mammary tumors in Sprague-Dawley rats by combination of lysine, proline, arginine, ascorbic acid and green tea extract. Breast Cancer Res 7:R291–R295.

Taper HS, Jamison JM, Gilloteaux J, Summers JL, Calderon PB. 2004. Inhibition of the development of metastases by dietary vitamin C:K3 combination. Life Sci 75:955–967.

Trakul N, Rosner MR. 2005. Modulation of the MAP kinase signaling cascade by Raf kinase inhibitory protein. Cell Res 15:19–23.

Wybieralska E, Koza M, Sroka J, Czyz J, Madeja Z. 2008. Ascorbic acid inhibits the migration of Walker 256 carcinosarcoma cells. Cell Mol Biol Lett 13:103–111.

Yang SH, Kim JS, Oh TJ, Kim MS, Lee SW, Woo SK, Cho SH, Chio YH, Kim YH, Rha SW, Chung HC, An SW. 2003. Genome-scale analysis of resveratrol-induced gene expression profile in human ovarian cancer cells using a cDNA microarray. Int J Oncol 22:741–750.

Yeung K, Seitz T, Li S, Janosch P, McFerran B, Kaiser C, Fee F, Katsanakis KD, Rose DW, Mischak H, Sedivy JM, Kolch W. 1999. Suppression of Raf-1 kinase activity and MAP kinase signalling by RKIP. Nature 401:173–177.

Yeung KC, Rose DW, Dhillon AS, Yaros D, Gustafsson M, Chatterjee D, McFerran B, Wyche J, Kolch W, Sedivy JM. 2001. Raf kinase inhibitor protein interacts with NF-kappaB-inducing kinase and TAK1 and inhibits NF-kappaB activation. Mol Cell Biol 21:7207–7217.